Vol. 36 (2005) *ACTA PHYSICA POLONICA B* No 4

VIBRATIONAL AND ROTATIONAL SEQUENCES IN ^{101}Mo AND ^{103,4}Ru STUDIED VIA MULTINUCLEON TRANSFER REACTIONS*

P.H. Regan[a,b], C. Wheldon[a,c], A.D. Yamamoto[a,b]
J.J. Valiente-Dobón[a,d], D. Cline[e], C.Y. Wu[e], A.O. Macchiavelli[f]
F.R. Xu[g], J.F. Smith[h], K. Andgren[a,i], R.S. Chakrawarthy[h,j]
M. Cromaz[f], P. Fallon[f], S.J. Freeman[h], A. Gorgen[f], A. Hayes[e]
H. Hua[e], S.D. Langdown[a,b], I-Y. Lee[f], C.J. Pearson[a,j]
Zs. Podolyák[a] and R. Teng[e]

[a]Dept. of Physics, University of Surrey, Guildford, GU2 7XH, UK
[b]WNSL, Yale University, New Haven, CT 06520-8124, USA
[c]Hahn-Meitner-Institute, Glienicker Strasse 100, 14109 Berlin, Germany
[d]Dept. of Physics, University of Guelph, Ontario, N1G 2W1, Canada
[e]Dept. of Physics, University of Rochester, Rochester, NY 14627, USA
[f]Lawrence Berkeley National Laboratory Berkeley, CA 94720, USA
[g]Dept. of Technical Physics, Peking University, Beijing, 100871, China
[h]Dept. of Physics and Astronomy, University of Manchester, M13 9PL, UK
[i]Royal Institute of Technology, Dept. of Physics, 106 91 Stockholm, Sweden
[j]TRIUMF, 4004 Westbrook Mall, Vancouver, BC, V6T 2A3, Canada

(Received November 30, 2004)

The near-yrast states of $^{101}_{42}Mo_{59}$ and $^{103,4}_{44}Ru_{59,60}$ have been studied following their population via heavy-ion multinucleon transfer reactions between a ^{136}Xe beam and a thin, self-supporting ^{100}Mo target. The ground state sequence in ^{104}Ru can be understood as demonstrating a simple evolution from a quasi-vibrational structure at lower spins to statically deformed, quasi-rotational excitation involving the population of a pair of low-Ω $h_{11/2}$ neutron orbitals. The effect of the decoupled $h_{11/2}$ orbital on this vibration-to-rotational evolution is demonstrated by an extension of the "E-GOS" prescription to include odd-A nuclei. The experimental results are also compared with self-consistent Total Routhian Surface calculations which also highlight the polarising role of the highly aligned neutron $h_{11/2}$ orbital in these nuclei.

PACS numbers: 21.10.–k, 21.10.Re, 23.20.Lv, 27.60.+j

* Presented at the XXXIX Zakopane School of Physics — International Symposium "Atomic Nuclei at Extreme Values of Temperature, Spin and Isospin", Zakopane, Poland, August 31–September 5, 2004.

1. Introduction

The study of near-stable and neutron-rich nuclei with medium to heavy mass has been revolutionised by the advent of high-efficiency gamma-ray spectrometer arrays which allow gates to be set on multi-dimensional gamma-ray energy arrays, thereby selecting rather weakly populated reaction channels. The initial proponents of this method, led by Broda and collaborators utilised the thick or backed target technique when studying such binary reactions [1–3]. This has the great advantage of minimising the degradation of the spectral lineshape due to Doppler effects. However, this method restricts the angular momenta which can be studied discretely in such reactions to states with effective decay half-lives which are longer than the slowing-down time of the reaction products in the target and/or backing, typically the order of a few picoseconds.

This paper describes recent work to study the structure of near-stable and slightly neutron-rich nuclei around $A \sim 100$ with multinucleon transfer reactions using a thin, self-supporting target and making event-by-event Doppler corrections on the individual reaction products. Further details of this work can be found in references [4–6].

2. Experimental details, data analysis and results

The nuclei of interest were populated using heavy-ion binary reactions between a self-supporting, (420μ g/cm^2) ^{100}Mo target and a ^{136}Xe beam at a laboratory energy of 700 MeV. The beam was provided by the 88" cyclotron at the Lawrence Berkeley National Laboratory and had a natural pulsing of approximately $2 \rightarrow 3$ ns width, separated by 64 ns with typical, on-target beam currents of $1 \rightarrow 2p$ nA. Reaction γ rays were detected using the GAMMASPHERE array [7], which in this experiment consisted of 102 Compton-suppressed hyperpure germanium detectors. The binary fragments were detected using the position-sensitive gas-filled detector, CHICO [8,9], which enabled an event-by-event Doppler correction to be applied to the raw γ-ray data. The detection of co-planar events in CHICO allowed the separation of both beam-like (BLF) and target-like fragments (TLF) by the measurement of their position relative to the beam direction. The angle-dependent velocity of the target-like fragments was calculated assuming 2-body kinematics to vary between 3% and 11% of the speed of light.

The acquisition master trigger required that at least three prompt, Compton-suppressed γ rays were detected in GAMMASPHERE within approximately 50 ns of each other, together with two co-planar binary fragments in CHICO. The hevimet collimators were removed from the GAMMASPHERE Compton-suppression shields, thereby allowing a measure of the total reaction γ-ray fold associated with each event to be made [4–6].

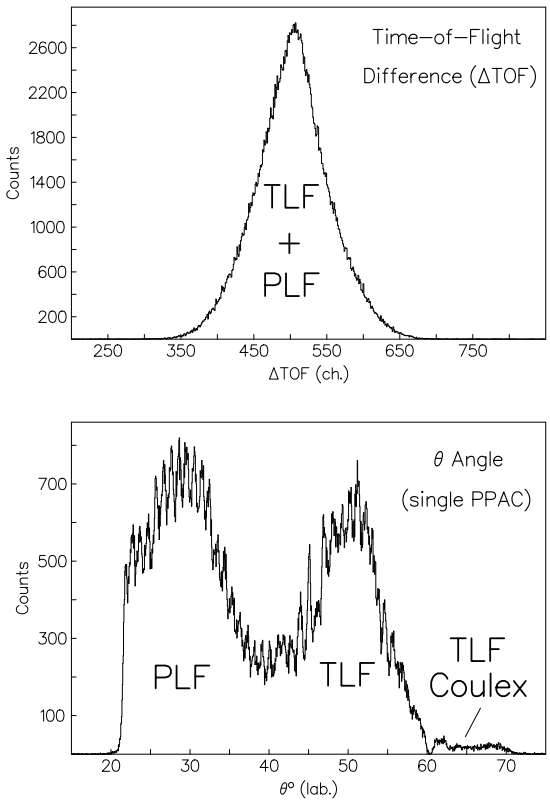

Fig. 1. Examples of partial statistics total projections of the time-of-flight difference and azimuthal angle of the binary fragments following the ^{100}Mo+^{136}Xe reaction as discussed in the text.

The data were sorted into standard γ-ray energy coincidence matrices and cubes which were subsequently analysed using the RADWARE package [10]. A total of 9×10^8 suppressed germanium triples and higher fold events were detected in coincidence with two, co-planar binary fragments during the course of a four day experiment.

Fig. 1 shows the total projections of the time of flight difference and the azimuthal angle of the binary fragments as measured with this mastergate condition. Using the temporal separation between prompt Doppler-shifted transitions which feed isomeric states and those transitions which depopulate such isomers and decays from fragments stopped in the CHICO detector, time-correlated spectroscopy could be performed (see references [5, 11, 12] for details). In this way delayed gates were set on transitions depopulating the $I^\pi = (11/2)^-$ isomeric state in ^{101}Mo [13] and the prompt transitions above the isomer could be clearly identified (see Fig. 2).

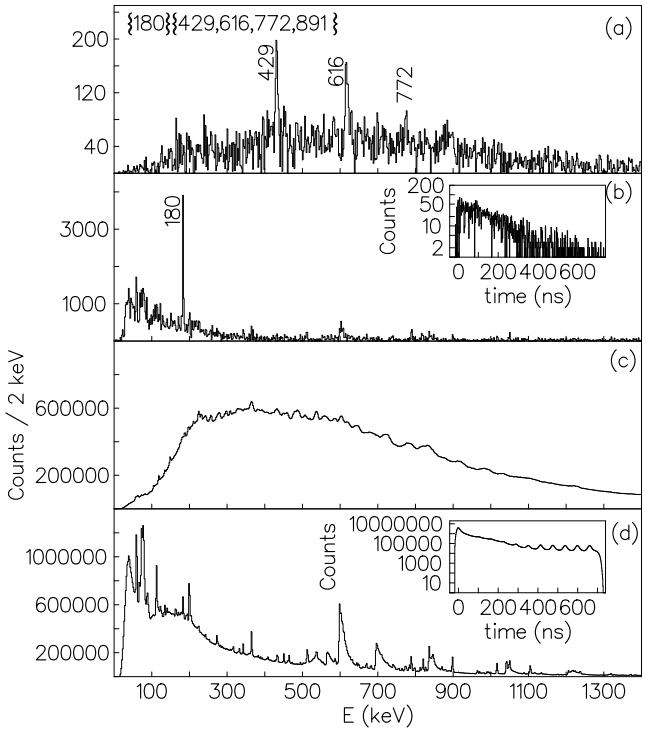

Fig. 2. Isomer gating identifying the states built on the $I^{\pi} = (11/2)^{-}$ isomer in ^{101}Mo. (a) shows the sum of double gates between the prompt transitions identified in coincidence with the delayed (*i.e.*, $50 \rightarrow 200$ ns after the prompt master trigger) 180 keV transition in ^{101}Mo. The delayed gamma-ray at 180 keV corresponds to the $(5/2)^{+} \rightarrow (1/2)^{+}$ transition decaying from the level at 239 keV in ^{101}Mo [13]. Its delayed projection, in coincidence with prompt transitions at 429, 616, 772 and 891 keV is shown in part (b), together with the summed time-difference spectra between the prompt 429, 616, 772 and 891 keV decays and the delayed 180 keV transition, which yields a half-life for this isomer of 95 ± 15 ns. The spectra in parts (c) and (d) show the γ-ray total projections gated on prompt and delayed time regions, respectively.

Examples of spectra generated from this analysis which show the decoupled neutron $h_{11/2}$ bands in the $N = 59$ isotones ^{101}Mo and ^{103}Ru [14], together with the yrast sequence in ^{104}Ru [3] are shown in Figs. 2 and 3 with the relevant partial decay schemes for these nuclei given in Fig. 4. The energies of the transitions and their mutually coincident "in-band" nature are consistent with similar E2 cascades observed built on the yrast and decoupled bands (assigned as being built on the $[550]\,1/2^{-}$ Nilsson orbital) in the neighboring isotones and isotopes [15, 16].

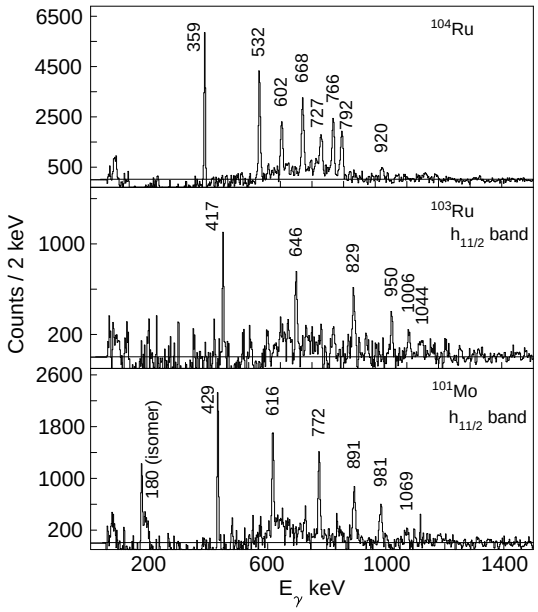

Fig. 3. Figure particle gated, summed double-gated gamma-ray spectra showing the yrast sequence in ^{104}Ru and the decoupled $\nu h_{11/2}$ band structures in ^{101}Mo and ^{103}Ru. The gamma-ray energy uncertainties in these spectra are approximately ± 2 keV.

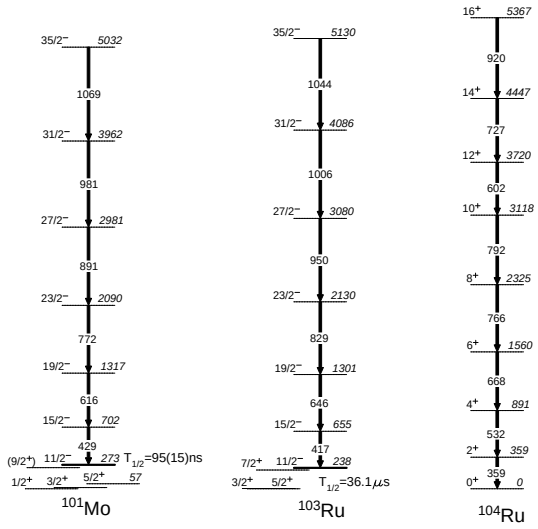

Fig. 4. Partial decay schemes for ^{103,4}Ru and ^{101}Mo as determined from the ^{136}Xe $+^{100}$Mo reaction using CHICO+GAMMASPHERE. The typical gamma-ray energy uncertainty in these decay schemes is approximately ± 2 keV from the present work.

The identification of the negative-parity decoupled band in ^{101}Mo completes the systematics for this region, which are shown in Fig. 5. These suggest a systematically low ($\beta \sim 0.15 \rightarrow 0.2$) value for the quadrupole deformation for these structures. Note that the recent studies by Hua *et al.*, [9] of the $N = 61$ isotones in this region suggest a large increase in the quadrupole deformation of these nuclei compared to the $N = 59$ isotopes studied in the present work.

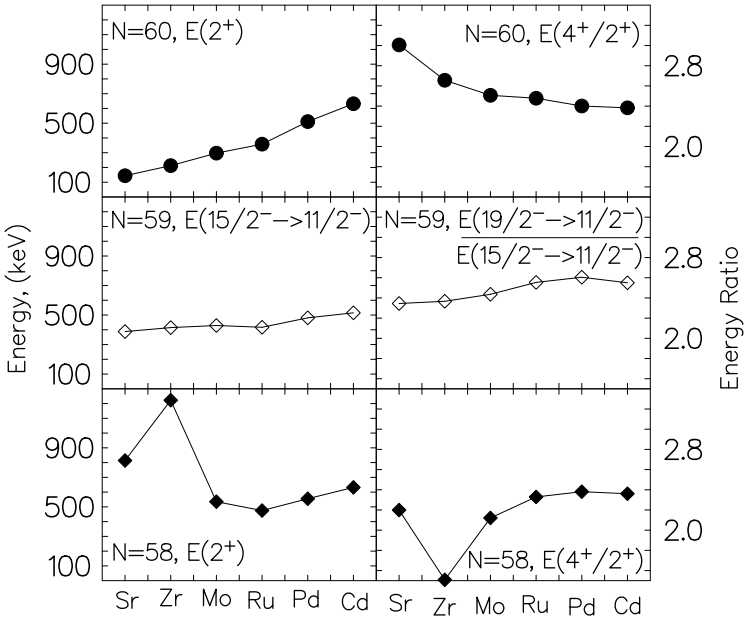

Fig. 5. Excitation energy and energy ratio systematics for the even Z, $N = 58$ and 60 isotones and the decoupled $h_{11/2}$ neutron structures in the $N = 59$ isotonic chain from strontium ($Z = 38$) to cadmium ($Z = 48$) including the new data point for ^{101}Mo.

2.1. Rotational and vibrational competition around $A \sim 100$

The concept of the E-Gamma Over Spin or E-GOS prescription has been applied to a number of even–even nuclei around the $A \sim 100$ region [17, 18] with the conclusion that many of these nuclei exhibit a decay sequence consistent with quasi-vibrational excitations at lower spins, which gives way to more statically (albeit weakly) deformed sequences above spins of $10\hbar$. This change in structure is generally interpreted [18] as being associated with the population of $h_{11/2}$ neutron orbitals (which reside low in the shell) and their prolate-shape-polarising effect or "stiffening" of the nuclear mean field.

The question of how to deal with odd-A systems in the E-GOS prescriptions can be addressed by substituting the spin (I) by a normalised spin minus the bandhead spin projection on the axis of symmetry, K, such that $I \rightarrow (I-K)$. For good rotors, the E-GOS prescription for odd-A systems then becomes [6]

$$R(I) \;=\; \frac{E_\gamma}{I} \rightarrow \frac{\hbar^2}{2\mathcal{J}}\frac{(4I-2)}{I} \rightarrow \frac{\hbar^2}{2\mathcal{I}}\frac{[4(I-K)]-2}{(I-K)}\,, \qquad (1)$$

$$R(I-K) \;=\; \frac{E_\gamma - \left(4K\frac{\hbar^2}{2\mathcal{J}}\right)}{I-K} = \frac{E_\gamma - KR_{K+2}}{I-K}\,. \qquad (2)$$

Fig. 6 shows the E-GOS plots for the $N = 57$ and 59 isotones ^{99,101}Mo and ^{101,103}Ru [15] and compares these with the yrast sequences in ^{100,2}Mo and ^{102,4}Ru. The E-GOS plots imply an evolution from vibrational to rotational excitations in the positive-parity structures in the $N = 57$ isotone ^{101}Ru [15], which mirrors the yrast sequences in the nearby even–even nuclei ^{100}Mo and ^{104}Ru. By contrast, the E-GOS plots for the decoupled

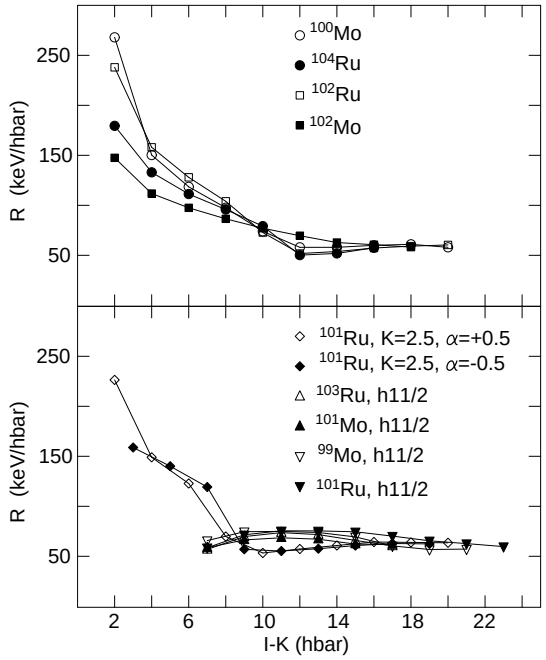

Fig. 6. (Upper) E-GOS plots for the yrast, ground-state sequences in ^{100,2}Mo and ^{102,4}Ru. (Lower) E-GOS plots for the decoupled $h_{11/2}$ bands in ^{99,101}Mo and ^{101,103}Ru (assuming $K = 1/2$ in all cases.) The two signatures of the $K = (5/2)^+$ band in ^{101}Ru [15] are also shown for comparison.

$h_{11/2}$ sequences for ^{99,101}Mo and ^{101,103}Ru demonstrate loci consistent with a rotational-like behaviour directly from the bandhead.

The recent report on the structure of the heavier Mo istones [9] suggests a significant increase in the core quadrupole deformation for these nuclei compared to the $N = 59$ isotones, consisent with the considerable difference in behaviour in the yrast sequence for ^{102}Mo compared to ^{100}Mo. The increase in core deformation observed in going from neutron number 58 to neutron number 60 is well documented in this region [19–21]. Since the current work highlights both the rotational nature and the rather weakly deformed status of the odd-parity structure in ^{101}Mo, our data suggest that this jump is indeed due to the effect of the $N = 60$ deformed shell gap and a change in core deformation, rather than the intrinsic deformation driving properties of the neutron $h_{11/2}$ orbitals as has been suggested elsewhere in the literature [20].

2.2. Comparison with TRS calculations

In order to compare the experimental data with theoretical predictions in the bandcrossing region, the effect of collective rotation on the microscopic structures in ^{101}Mo and ^{103}Ru were investigated in the framework of the Cranked–Woods–Saxon–Strutinsky model by means of Total-Routhian-Surface (TRS) calculations in a three-dimensional deformation $(\beta_2, \beta_4, \gamma)$ space (see reference [15] and references therein for details).

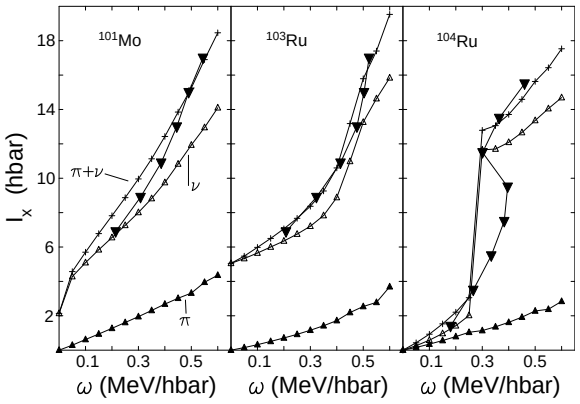

Fig. 7. Comparison between the experimentally derived total aligned angular momentum in the $h_{11/2}$ decoupled bands in ^{101}Mo and ^{103}Ru with self-consistent Total Routhian Surface calculations for the lowest energy negative parity, $\alpha = -1/2$ configurations in these nuclei. In each case the calculations show both the proton (π) and neutron (ν) contributions to the predicted total aligned angular momentum (I_x). A K-value of 1/2 has been assumed for these structures. The yrast sequence in the neighboring even–even core of ^{104}Ru has also been shown for comparison. In all cases, the experimental data are the large black triangles.

Fig. 7 shows the results of these calculations, which in general show good agreement, with the majority of the aligned angular momentum in each case being predicted to be generated by ($h_{11/2}$) neutron configurations. The dramatic effect of the $(\nu h_{11/2})^2$ crossing on the yrast structure in ^{104}Ru is well known in the region [3]. The fact that this crossing is blocked in the decoupled sequences in ^{101}Mo and ^{103}Mo can be taken as ample evidence for the $h_{11/2}$ character of their intrinsic structure.

3. Summary and conclusions

In summary, thin-target multinucleon transfer reactions have been utlised to identify and extend the yrast sequences in ^{101}Mo and ^{103,4}Ru. A decoupled structure, based on the neutron $h_{11/2}$ orbital has been identified in ^{101}Mo for the first time, completing the systematics of such excitations for the $N = 59$ isotones between Sr ($Z = 38$) and Cd ($Z = 48$). The results are compared with TRS calculations and interpreted using the E-GOS prescription, modified for use with odd-A nuclei. Both of these analyses highlight the role of the low-Ω $h_{11/2}$ intruder orbital in stabilising the quadruople deformation in this region.

This work is supported by EPSRC (UK) and the US Department of Energy, under grants DE-FG02-91ER-40609 and DE-AC03-76SF00098 and by the National Science Foundation. PHR acknowledges support from Yale University via both the Flint and the Science Development Funds. ADY, JJVD and SDL acknowledge the receipt of EPSRC postgraduate studentships. ZP acknowledges an EPSRC Advanced Fellowship. FRX acknowledges support from the Major State Basic Research Development Program of China (G2000077400) and the Chinese Ministry of Education. CW would like to thank the Alexander von Humboldt Foundation for their support.

REFERENCES

[1] J. Wrzesinski *et al., Eur. Phys. J.* **A20**, 57 (2004); B. Fornal *et al., Phys. Rev.* **C67**, 034318 (2003); W. Krolas *et al., Nucl. Phys.* **A724**, 289 (2003); B. Fornal *et al., Phys. Rev. Lett.* **87**, 212501; C.T. Zhang *et al., Phys. Rev.* **C62**, 057305 (2000); R. Broda *et al., Phys. Rev.* **C59**, 3071 (1999); B. Fornal *et al., Phys. Rev.* **C55**, 762 (1997); R. Broda *et al., Phys. Rev. Lett.* **74**, 868 (1995); R.H. Meyer *et al., Phys. Lett.* **336B**, 308 (1994); B. Fornal *et al., Phys. Rev.* **C49**, 2413 (1994); R. Broda *et al., Phys. Rev. Lett.* **68**, 1671 (1992); R. Broda *et al., Phys. Lett.* **251B**, 245 (1990); J.F.C. Cocks *et al., J. Phys.* **G26**, 23 (2000); A.N. Wilson *et al., Eur. Phys. J.* **A9**, 183 (2000); S. Mohammadi *et al.*, *Brazillian J. Phys.* **34**, 792 (2004); Zs. Podolyák *et al., Int. J. Mod. Phys.* **E13**, 123 (2004); Y.H. Zhang *et al., Phys. Rev.* **C70**, 024301 (2004); C. Wheldon *et al., Phys. Lett.* **425B**, 239 (1998).

[2] R. Broda *et al., Phys. Rev.* **C49**, 2413 (1994).
[3] P.H. Regan *et al., Phys. Rev.* **C55**, 2305 (1997).
[4] P.H. Regan *et al., AIP Conf. Proc.* **701**, 329 (2003).
[5] P.H. Regan *et al., Phys. Rev.* **C68**, 044313 (2003).
[6] P.H. Regan *et al., AIP Conf. Proc.* **726**, 157 (2004).
[7] I.Y. Lee, *Nucl. Phys.* **A520**, 641c (1990).
[8] M.W. Simon *et al., Nucl. Instrum. Methods Phys. Res.* **A452**, 205 (2000).
[9] H. Hua *et al., Phys. Rev.* **C69**, 014317 (2004).
[10] D.C. Radford, *Nucl. Instrum. Methods Phys. Res.* **A361**, 297 (1995).
[11] J.J. Valiente-Dobón *et al., Phys. Rev.* **C69**, 024316 (2004).
[12] P.H. Regan *et al., Laser Phys. Lett.* **1**, 317 (2004).
[13] W. Booth *et al., Phys. Lett.* **30B**, 335 (1969); W.L. Sievers *et al., Phys. Rev.* **C6**, 1001 (1972); H. Weigmann *et al., Phys. Rev.* **C20**, 115 (1979).
[14] N. Fotiades *et al., Phys. Rev.* **C58**, 1997 (1998).
[15] A.D. Yamamoto *et al., Phys. Rev.* **C66**, 024302 (2002).
[16] P.H. Regan *et al., J. Phys.* **G19**, L157 (1993).
[17] P.H. Regan *et al., Phys. Rev. Lett.* **90**, 152502 (2003).
[18] P.H. Regan *et al., AIP Conf. Proc.* **656**, 422 (2002).
[19] P. Federman, S. Pittel, *Phys. Lett.* **77B**, 29 (1977); *Phys. Rev.* **C20**, 920 (1979).
[20] W. Urban *et al., Nucl. Phys.* **A689**, 605 (2001).
[21] G. Lhersonneau *et al., Phys. Rev.* **C49**, 1379 (1994).